

Heme Protein Oxygen Affinity Regulation Exerted by Proximal Effects

Luciana Capece, Marcelo A. Marti, Alejandro Crespo, Fabio Doctorovich, and Darío A. Estrin*

Contribution from the Departamento de Química Inorgánica, Analítica y Química Física/ INQUIMAE-CONICET, Facultad de Ciencias Exactas y Naturales, Universidad de Buenos Aires, Ciudad Universitaria, Pabellón 2, Buenos Aires, C1428EHA, Argentina

Received March 23, 2006; E-mail: dario@qi.fcen.uba.ar

Abstract: Heme proteins are found in all living organisms and are capable of performing a wide variety of tasks, requiring in many cases the binding of diatomic ligands, namely, O₂, CO, and/or NO. Therefore, subtle regulation of these diatomic ligands' affinity is one of the key issues for determining a heme protein's function. This regulation is achieved through direct H-bond interactions between the bound ligand and the protein, and by subtle tuning of the intrinsic heme group reactivity. In this work, we present an investigation of the proximal regulation of oxygen affinity in Fe(II) histidine coordinated heme proteins by means of computer simulation. Density functional theory calculations on heme model systems are used to analyze three proximal effects: charge donation, rotational position, and distance to the heme porphyrin plane of the proximal histidine. In addition, hybrid quantum-classical (QM-MM) calculations were performed in two representative proteins: myoglobin and leghemoglobin. Our results show that all three effects are capable of tuning the Fe–O₂ bond strength in a cooperative way, consistently with the experimental data on oxygen affinity. The proximal effects described herein could operate in a large variety of O₂-binding heme proteins—in combination with distal effects—and are essential to understand the factors determining a heme protein's O₂ affinity.

Introduction

Heme proteins, the family of proteins containing the iron protoporphyrin (heme) cofactor, are found in all living organisms.^{1,2} They perform a wide variety of tasks ranging from electron transport³ and oxidation of organic molecules⁴ to the sensing and transport of small gaseous molecules, namely, O₂, CO, and NO.⁵ Out of these three ligands, O₂ is the most abundant and, at the same time, the one with the lowest affinity for free heme.^{5,6} The subtle regulation of oxygen affinity is therefore one of the key issues for determining a heme protein's function. In most heme proteins, the active site—where the oxygen can be bound—consists of a cavity on top of the heme group, known as the distal pocket. The iron atom is coordinated equatorially to the four nitrogens of the porphyrin macrocycle and axially to a fifth or proximal ligand under the heme ring, typically a histidine (His), cysteine (Cys), or tyrosine (Tyr) residue (Figure 1). Heme proteins that bind and transport oxygen (i.e., the classical globins, hemoglobin, and myoglobin)⁷ possess

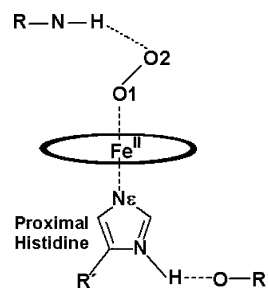


Figure 1. Oxygen binding site in Fe(II) histidine coordinated heme proteins.

the iron mainly in a pentacoordinated (5c) ferrous Fe^{II} high-spin configuration.⁸

Understanding environmental effects on the protein's affinity for oxygen has been a subject of great interest for many years.^{9,10} Many theoretical^{11,12} and experimental^{6,13,14} works have been

- (1) Kundu, S.; Trent, J. T., III; Hargrove, M. S. *Trends Plant Sci.* **2003**, *8*, 387–393.
- (2) Kadish, K. M.; Smith, K. M.; Guillard, R. *The Porphyrin Handbook*; Academic Press: San Diego, 2000; Vol. 4.
- (3) Simonneaux, G.; Bondon, A. *Chem. Rev.* **2005**, *105*, 2627–2646.
- (4) Shaik, S.; Kumar, D.; de Visser, S. P.; Altun, A.; Thiel, W. *Chem. Rev.* **2005**, *105*, 2279–2328.
- (5) Jain, R.; Chan, M. K. *J. Biol. Inorg. Chem.* **2003**, *8*, 1–11.
- (6) Olson, J. S.; Phillips, G. N., Jr. *J. Biol. Inorg. Chem.* **1997**, *2*, 544–552.
- (7) Voet, D.; Voet, J. G. *Biochemistry*; John Wiley and Sons: New York, Chichester, Brisbane, Toronto, Singapore, 1995.

- (8) Estrin, D. A.; Scherlis, D. A. *Int. J. Quantum Chem.* **2002**, *87*, 158–166.
- (9) Perutz, M. F.; Fermi, G.; Luisi, B. *Acc. Chem. Res.* **1987**, *20*, 309–321.
- (10) Satoru, U.; Eich, R.; Shibayama, N.; Olson, J. S.; Morimoto, H. *J. Biol. Chem.* **1998**, *273*, 23150–23159.
- (11) (a) Rydberg, P.; Sigfridsson, E.; Ryde, U. *J. Biol. Inorg. Chem.* **2004**, *9*, 203–223. (b) Sigfridsson, E.; Ryde, U. *J. Inorg. Biochem.* **2002**, *91*, 101–115. (c) Tangen, E.; Svadberg, A.; Ghosh, A. *Inorg. Chem.* **2005**, *44*, 7802–7805. (d) Spiro, T. G.; Kozlowski, P. M. *Acc. Chem. Res.* **2001**, *34*, 137–144. (e) Sigfridsson, E.; Ryde, U. *J. Biol. Inorg. Chem.* **1999**, *4*, 99–110. (f) Scherlis, D. A.; Estrin, D. A. *J. Am. Chem. Soc.* **2001**, *123*, 8436–8437.
- (12) Phillips, G. N.; Teodoro, M. L.; Li, T.; Smith, B.; Olson, J. S. *J. Phys. Chem. B* **1999**, *103*, 8817–8829.
- (13) Milani, M.; Pesce, A.; Nardini, M.; Ouellet, H.; Ouellet, Y.; Dewilde, S.; Bocedi, A.; Ascenzi, P.; Guertin, M.; Moens, L.; Friedman, J. M.; Wittenberg, J. B.; Bolognesi, M. *J. Inorg. Biochem.* **2005**, *99*, 97–109.

devoted to the investigation of distal effects, namely, the stabilization of bound oxygen by H-bond interactions with H-donor residues in the distal cavity.⁶ Usually, histidine, glutamine, tyrosine, or a combination of these residues^{13,15} found in the distal cavity perform this task. Consistently, a negative correlation between the electrostatic field in the distal cavity (determined mainly by the number and position of the H-bond donor groups) and the O₂ dissociation rate has been found in many heme proteins.¹² However, there are cases in which O₂ affinities do not follow the expected trends corresponding to the characteristics of the distal cavity. The paradigmatic examples of this behavior are the leghemoglobins.¹⁶

Leghemoglobins are monomeric heme protein members of the globin superfamily, found in the root nodules of leguminous plants that participate in nitrogen fixation.¹ It has been proposed that leghemoglobins' function is to facilitate oxygen diffusion from the root to the aerobes inside the nodule. As in mammalian globins, such as myoglobin (Mb), leghemoglobins present a histidine residue in the distal cavity. Unexpectedly and contrary to what is observed in Mb, site-directed mutagenesis studies showed that in soybean leghemoglobin (Lba) this residue does not significantly contribute to O₂ stabilization.¹⁶ Changing the distal histidine (HisE7) in Mb to non-H-bonding residues increases the dissociation rate constant more than 100-fold in all cases, whereas the same mutants in Lba have little (5-fold increase) or no effect. Still, the oxygen affinity displayed by Lba is even larger than the one observed in Mb, as evidenced from its smaller dissociation constant (k_{off} values of 5.6 and 15 s⁻¹ for Lba and Mb, respectively).¹

Possible causes for the unusual results mentioned above are proximal effects that could also modulate the oxygen affinity.¹⁷ These effects may be due to the charge relay mechanism¹⁸ and/or to the rotational position of the proximal histidine.¹⁹ The charge relay mechanism consists of the hydrogen bonding network that tunes the basicity of the proximal histidine and therefore modulates its charge transfer capacity to the iron,²⁰ which in turn stabilizes the iron oxygen bond through π -back-donation from the iron.²¹ The rotational position of the histidine, defined as the position of the plane containing the imidazole group of the proximal histidine relative to the line that goes through two opposite pyrrolic nitrogens, has also been proposed as an O₂ bond modulation mechanism. If the plane is aligned with this line, the conformation is called "eclipsed", but if it forms an angle of 45°, it is called "staggered" (see Figure 2). X-ray crystallography of both heme proteins showed that, in Mb, the imidazole ring is in the eclipsed conformation,²² while in Lba, it is closer to the staggered conformation.²³ This fact has been hypothesized to enhance ligand affinity through the

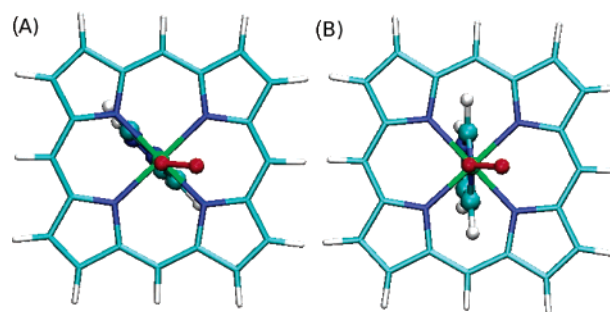


Figure 2. Histidine rotational position: (A) eclipsed and (B) staggered.

proximal side for Lba and not for Mb.¹⁷ In order to support this hypothesis, mutants in which the proximal histidine is changed to glycine and imidazole is added to occupy the proximal position were performed. The mutant proteins displayed a \sim 3-fold increase in the k_{off} for Lba and a \sim 3-fold decrease for Mb.¹⁷

In addition, a third, but up to now, neglected mechanism for proximal regulation of oxygen affinity could be the control of the distance between the proximal histidine and the Fe of the heme group. In heme proteins, the proximal histidine is anchored to the protein scaffold through the covalent C α –C β bond and also through H-bond interactions, as mentioned above. Through these interactions, the protein is able to constrain the position of the histidine relative to the heme group and, therefore, modulate oxygen affinity.

In this work, we have characterized the proximal affinity regulation mechanism operative in heme proteins by means of density functional theory (DFT) calculations on porphyrin model systems. We analyzed the three main factors controlling proximal regulation: the charge relay mechanism, the proximal histidine rotational position, and the distance between the proximal histidine and the Fe atom. In addition, we have also performed hybrid quantum-classical (QM-MM) calculations of oxygen affinity for wild-type and selected mutants of Mb and Lba to provide a complete picture of oxygen affinity modulation through proximal effects.

Computational Methods

In order to characterize the proximal affinity regulation effects, we have performed QM and QM-MM calculations of the O₂ binding energy (ΔE_{O_2}), which is defined as

$$\Delta E_{\text{O}_2} = E_{\text{Heme-O}_2} - E_{\text{O}_2} - E_{\text{Heme}}$$

where $E_{\text{Heme-O}_2}$ is the energy of the oxy heme complex, E_{Heme} is the energy of the free heme group, and E_{O_2} is the energy of the isolated oxygen molecule. The ferrous O₂ complex was treated as a low spin singlet state, which is known to be the ground state for this system. The ferrous unbound pentacoordinated heme group was treated as a high-spin quintuplet state.⁸ For clarity purposes, in some cases, the O₂ binding energy of a selected constrained conformation is given using the equilibrium binding energy as a reference. We named this relative energy ΔE_{comp} .

$$\Delta E_{\text{comp}} = \Delta E_{\text{O}_2(\text{constrained})} - \Delta E_{\text{O}_2(\text{equilibrium})}$$

- (14) Cutruzzolà, F.; Travaglini Allocatelli, C.; Ascenzi, P.; Bolognesi, M.; Sligar, S. G.; Brunori, M. *FEBS Lett.* **1991**, *282*, 281–284.
 (15) Kloek, A. P.; Yang, J.; Mathews, F. S.; Goldberg, D. E. *J. Biol. Chem.* **1993**, *268*, 17669–17671.
 (16) Kundu, S.; Blouin, G. C.; Premer, S. A.; Sarath, G.; Olson, J. S.; Hargrove, M. S. *Biochemistry* **2004**, *43*, 6241–6252.
 (17) Kundu, S.; Snyder, B.; Das, K.; Chowdhury, P.; Park, J.; Petrich, J. W.; Hargrove, M. S. *Proteins* **2002**, *46*, 268–277.
 (18) Franzen, S. *J. Am. Chem. Soc.* **2001**, *123*, 12578–12589.
 (19) Narula, S. S.; Dalvit, C.; Appleby, C. A.; Wright, P. E. *Eur. J. Biochem.* **1988**, *178*, 419–435.
 (20) (a) Goodin, D. B.; McRee, D. E. *Biochemistry* **1993**, *32*, 3313–3324. (b) Vogel, K. M.; Spiro, T. G.; Shelver, D.; Thorsteinsson, M. V.; Roberts, G. P. *Biochemistry* **1999**, *38*, 2679–2687.
 (21) Oertling, W. A.; Kean, R. T.; Wever, R.; Babcock G. T. *Inorg. Chem.* **1990**, *29*, 2633–2645.
 (22) Quillin, M. L.; Arduini, R. M.; Olson, J. S.; Phillips, G. N., Jr. *J. Mol. Biol.* **1993**, *234*, 140–155.

- (23) Hargrove, M. S.; Barry, J. K.; Brucker, E. A.; Berry, M. B.; Phillips, G. N., Jr.; Olson, J. S.; Arredondo-Peter, R.; Dean, J. M.; Klucas, R. V.; Sarath, G. *J. Mol. Biol.* **1997**, *266*, 1032–1042.

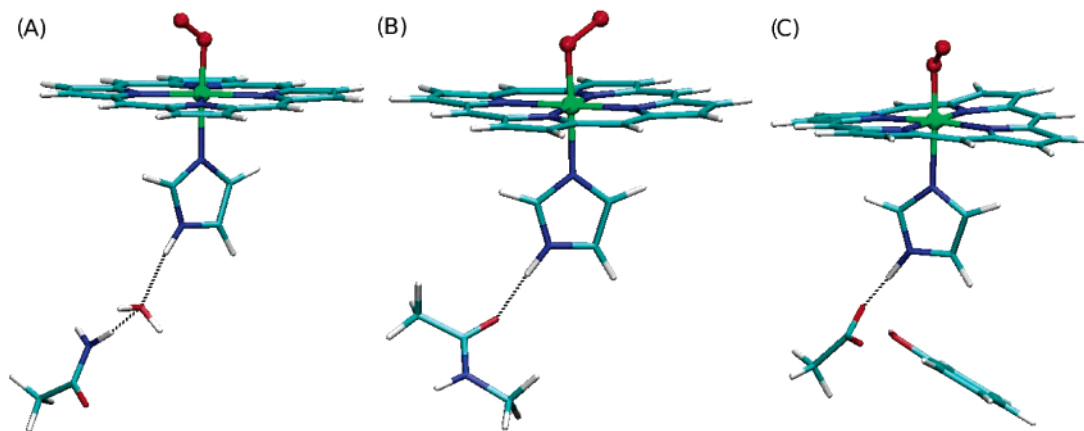


Figure 3. Model systems representing (A) Fix-L, (B) Hb β , and (C) Hrp.

In the first place, we investigated the charge relay mechanism by comparing the O₂ binding energies for four selected model systems. These model systems include the Fe–porphyrin group with an imidazole ring bound to the Fe by the N ϵ , representing the proximal His. Three of them also included different additional moieties, which interact with the δ -hydrogen of histidine, as depicted in Figure 3a–c. These chosen ligands, which span a wide range in H-bonding capacity, mimic the proximal sites of Fix-L,²⁴ hemoglobin β subunit (Hb β),²⁵ and horse radish peroxidase (Hrp),²⁶ respectively. In the Fix-L model, we included a water molecule that establishes a H-bond with the His and an acetamide molecule. In Hb β , the H-bond is formed with an amide carbonyl group, and in Hrp, we included an acetate group and a phenol molecule. In the three cases, the heavy atoms of the extra groups were fixed during the simulations, in order to maintain the original protein's conformation. The use of diffuse functions is known to be important in the description of H-bond interactions.²⁷ In order to analyze the effect of the inclusion of diffuse functions in the observed trends, we recalculated the O₂ binding energy for the three model systems, adding diffuse functions for nitrogen, oxygen, and hydrogen atoms. More computational details can be found in the Supporting Information.

In the second place, we have investigated the role of the proximal histidine rotational position on the O₂ affinity, by calculating the O₂ binding energies for staggered and eclipsed histidine conformations (Figure 2). The calculations were performed in two different model systems, one including the Fe–porphyrin group and an imidazole group coordinated by the N ϵ to the Fe (representing the proximal histidine), and another adding an acetone molecule coordinated to the δ -hydrogen of histidine. We have computed the O₂ affinity for both conformations by restraining the dihedral angle to the desired value.²⁸

In order to investigate the influence of possible restraints on the distance between the proximal histidine and the Fe atom, we have performed QM calculations of the O₂ binding energy as a function of the distance between the proximal histidine and the porphyrin plane. The model system used in this case was a Fe–porphyrin group and an imidazole group. The calculations were performed by calculating the O₂ binding energy for fixed distances between the N ϵ of the imidazole and the porphyrin plane defined as the center of the four N_{porphyrin} atoms coordinated to the Fe atom. The Fe atom was free to move during the simulations. We computed also E_{O_2} at the Fe–His equilibrium distance (i.e., the fully optimized model) as a reference.

In all cases, the QM calculations were performed at the density functional theory (DFT) level with the SIESTA code.²⁹ DFT methods, including the SIESTA code, have shown an excellent performance for medium and large systems and have also proven to be appropriate for biomolecules and, specifically, for heme models.^{8,30–32} The use of standard norm-conserving pseudopotentials³³ avoids the computation of core electrons, smoothing at the same time the valence charge density. In our study, the nonlinear partial-core correction³⁴ is applied to the iron atom. Basis functions consist of localized (numerical) pseudoatomic orbitals, projected on a real space grid to compute the Hartree potential and exchange correlation potentials' matrix elements. For all atoms, basis sets of double plus polarization quality were employed, with a pseudoatomic orbital energy shift of 25 meV and a grid cutoff of 150 Ry.²⁹ Calculations were performed using the generalized gradient approximation functional proposed by Perdew, Burke, and Ernzerhof.³⁵ This combination of functional and basis sets has been already validated for heme models.^{31,32}

Finally, in order to provide a more complete picture of oxygen affinity modulation through proximal effects, we performed QM-MM calculations on myoglobin and leghemoglobin. For both proteins, we calculated the O₂ binding energy for the wild-type proteins and three mutants: the distal mutant HisE7xGly, the proximal mutant HisF8xGly, in which we have included an imidazole coordinated to the heme moiety and the double mutant HisE7xGly and HisF8xGly (plus imidazole). The mutant proteins were constructed in silico. In these complex systems, predictions based on total potential energy differences may present flaws because motions in regions distant to the active site during minimizations may affect significantly the energy.³⁶ This is a key issue in our problem since the differences in O₂ affinity due to proximal effects are very small, as evidenced in the small differences in the k_{off} values obtained by site-directed mutagenesis experiments in Lba and Mb. In order to analyze the structural trends, we have performed full

(24) Gong, W.; Hao, B.; Mansy, S. S.; Gonzalez, G.; Gilles-Gonzalez, M. A.; Chan, M. K. *Proc. Natl. Acad. Sci. U.S.A.* **1998**, *95*, 15177–15182.
 (25) Liddington, R.; Derewenda, Z.; Dodson, E.; Hubbard, R.; Dodson, G. *J. Mol. Biol.* **1992**, *228*, 551–579.
 (26) Gajhede, M.; Schuller, D. J.; Henriksen, A.; Smith, A. T.; Poulos, T. L. *Nat. Struct. Biol.* **1997**, *4*, 1032–1038.
 (27) Rablen, P. R.; Lockman, J. W.; Jorgensen, W. L. *J. Phys. Chem. A* **1998**, *102*, 3782–3797.
 (28) Crespo, A.; Scherlis, D. A.; Martí, M. A.; Ordejón, P.; Roitberg, A. E.; Estrin, D. A. *J. Phys. Chem. B* **2003**, *107*, 13728–13736.

(29) Soler, J. M.; Artacho, E.; Gale, J. D.; García, A.; Junquera, J.; Ordejón, P.; Sánchez-Portal, D. *J. Phys.: Condens. Matter* **2002**, *14*, 2745–2779.
 (30) (a) Martí, M. A.; Crespo, A.; Bari, S. E.; Doctorovich, F. A.; Estrin, D. A. *J. Phys. Chem. B* **2004**, *108*, 18073–18080. (b) Guallar, V.; Friesner, R. A. *J. Am. Chem. Soc.* **2004**, *126*, 8501–8508. (c) Schoneboom, J. C.; Lin, H.; Reuter, N.; Thiel, W.; Cohen, S.; Oglario, F.; Shaik, S. *J. Am. Chem. Soc.* **2002**, *124*, 8142–8151. (d) Rovira, C.; Kunc, K.; Hutter, J.; Ballone, P.; Parrinello, M. *J. Phys. Chem. A* **1997**, *101*, 8914–8925.
 (31) (a) Martí, M. A.; Capece, L.; Crespo, A.; Doctorovich, F.; Estrin, D. A. *J. Am. Chem. Soc.* **2005**, *127*, 7721–7728. (b) Crespo, A.; Martí, M. A.; Kalko, S. G.; Morreale, A.; Orozco, M.; Gelpi, J. L.; Estrin, D. A. *J. Am. Chem. Soc.* **2005**, *127*, 4433–4444.
 (32) Martí, M.; Scherlis, D. A.; Doctorovich, F.; Ordejón, P.; Estrin, D. *J. Biol. Inorg. Chem.* **2003**, *8*, 595–600.
 (33) Troullier, N.; Martins, J. L. *Phys. Rev. B* **1991**, *43*, 1993–2006.
 (34) Louie, S. G.; Froyen, S.; Cohen, M. L. *Phys. Rev. B* **1982**, *26*, 1738–1742.
 (35) Perdew, J. P.; Burke, K.; Ernzerhof, M. *Phys. Rev. Lett.* **1996**, *77*, 3865–3868.
 (36) Crespo, A.; Martí, M. A.; Estrin, D. A.; Roitberg, A. E. *J. Am. Chem. Soc.* **2005**, *127*, 6940–6941.

QM-MM optimizations of the oxygenated proteins. In addition, and in order to estimate trends in the proximal effects, we have performed calculations of the vertical O_2 binding energy, defined as the difference between the QM-MM fully optimized oxy conformation and the deoxy structure frozen at the same geometry plus O_2 energies. The mutant O_2 binding energies are reported using the wild-type proteins as the reference.

We constructed initial structures for our calculations from the structures of the oxygenated Mb and Lba (PDB codes 2MGM²² and 1BIN,²³ respectively). Histidine protonation was assigned favoring H-bond formation. The systems were solvated with water molecules up to a distance of 30 Å of the heme center. All classical simulations were performed with the Amber8 package.³⁷ The whole systems were heated to 300 K, and a 500 ps molecular dynamics was performed to allow them to relax and equilibrate. Then the systems were cooled slowly to 0 K. The root-mean-square deviation (rmsd) of both proteins with respect to the X-ray structure resulted less than 1 Å during the MD simulations, indicating that the protein has not undergone any significant deviation from the original RX structure and that a reasonably good equilibration has been achieved. Full hybrid QM-MM geometry optimizations of the oxygenated wild-type and mutant proteins were performed using a conjugate gradient algorithm, using our own QM-MM implementation on the SIESTA code.²⁸ Only residues located less than 12 Å apart from the catalytic iron center were allowed to move freely. In order to obtain the vertical O_2 binding energy, we calculated the deoxygenated proteins frozen in the optimized oxygenated conformation. The QM subsystems were treated at the DFT level as described above, whereas the classical subsystems were treated using the Amber99 force field parametrization.³⁸ We have selected the iron porphyrinate plus the axial ligands as the quantum subsystem. The rest of the protein unit mentioned above and the water molecules were treated classically. The frontier between the QM and MM portions of the system has been treated by the scaled position link atom method.³⁹ Link atoms have been used in the proximal histidine to separate the QM-treated imidazole ring from the backbone of the amino acids and to separate the core of the porphyrin from its side chains.

Results and Discussion

As mentioned above, we analyzed the three different proximal effects related to the regulation of oxygen affinity in heme proteins. The O_2 binding energy (ΔE_{O_2}) values are related to the experimental dissociation rate constants (k_{off}).⁶ In this context, the comparative oxygen binding energy (ΔE_{comp}) provides an estimation of the relative oxygen affinity between the systems under comparison. We studied carefully selected

Table 1. Calculated Oxygen Affinities (ΔE_{O_2}), Charge Received by the O_2 (Δq_{O_2}) and Donated by the Imidazole Group Plus the Extra Groups of Each Model, When Corresponding (Δq_{prox}), and Experimental Fe– O_2 and Fe–His Raman Frequencies

	ΔE_{O_2} (kcal/mol)	Δq_{O_2} (e)	Δq_{prox} (e)	$\Delta E_{O_2}^a$ (kcal/mol)	ν_{Fe-His} (cm^{-1})	ν_{Fe-O_2} (cm^{-1})
isolated	22.2	−0.202	0.158	22.9	209 ^b	564 ^b
heme–imidazole complex						
Fix-L ⁴⁰	22.0	−0.197	0.160	22.7	210	569
Hb β ⁴¹	24.7	−0.248	0.200	25.3	220	572
Hrp ⁴²	18.5	−0.259	0.325	19.2	241	559

^a Values calculated using an extended basis (see Computational Methods.)

^b Data taken from (2M)Fe^{II}– O_2 (TPVPP),²¹ which is an isolated heme–imidazole model.

model systems which allowed us to obtain quantitative information on oxygen affinity for the three effects mentioned.

Contribution from the Charge Relay Mechanism. In a previous work, we showed that the strength of the H-bond between the H δ of the proximal histidine and the charge donated by the His to the Fe are positively correlated. Thus, as the strength of the H-bond increases, the His is able to donate more charge to the Fe atom.³² In our calculations, the amount of charge donated by the proximal His can be monitored by analyzing the resulting Mulliken populations for the imidazole group in the complex. Furthermore, the Mulliken populations of coordinated O_2 show the amount of charge received by the oxygen through π -backdonation.³² In order to analyze how the proximal His charge donation affects the oxygen affinity, we calculated the binding energy for three different model systems, as explained previously, in which the strength of the H-bond was different. Experimentally, the strength of the His–Fe bond (an indicator of the degree of charge donation from His to the iron) can be estimated from the His–Fe stretching frequency value³² and the Fe–O bond strength from the Fe– O_2 stretching frequency in the Fe(II)– O_2 complexes.

In Table 1, we present our calculations for the oxygen binding energy, the charge donated by the proximal imidazole, and the charge received by the O_2 for each protein model, together with the experimentally determined values for ν_{Fe-His} and ν_{Fe-O_2} for the corresponding proteins and an O_2 –porphyrin–imidazole complex. The results presented in Table 1 show that, as expected, when the hydrogen bond strength is increased (going down in Table 1), the charge donated by the histidine, the Fe–His bond strength (measured by the ν_{Fe-His}), and the charge received by the oxygen are increased concomitantly. However, the relationship between ΔE_{O_2} and the N δ –H-bond strength is not simple. The results for ΔE_{O_2} show that the affinity for oxygen has a maximum value when the strength of the hydrogen bond is intermediate, as that of a carbonyl H-bond acceptor. These results are fully consistent with the experimental data (ν_{Fe-O_2}) that show the same trend. This behavior can be explained in terms of a balance between the two oxygen–iron bonding effects (σ -donation and π -backdonation). The oxygen has a moderate σ -donation capacity and is a very good π -acceptor. As mentioned above, increasing the H-bond strength increases the charge available in the iron porphyrin system, and this is translated in more efficient π -backdonation (the O_2 becomes more negative) that increases the strength of the Fe–O bond. On the other hand, more charge in the iron porphyrin system reduces the σ -donation from the oxygen, weakening the

- (37) Pearlman, D. A.; Case, D. A.; Caldwell, J. W.; Ross, W. R.; Cheatham, T. E., III; DeBolt, S.; Ferguson, D.; Seibel, G.; Kollman, P. *Comp. Phys. Commun.* **1995**, *91*, 1–41.
- (38) Wang, J.; Cieplak, P.; Kollman, P. A. *J. Comput. Chem.* **2000**, *21*, 1049–1074.
- (39) (a) Eichinger, M.; Tavan, P.; Hutter, J.; Parrinello, M. *J. Chem. Phys.* **1999**, *110*, 10452–10467. (b) Rovira, C.; Schulze, B.; Eichinger, M.; Evansck, J. D.; Parrinello, M. *Biophys. J.* **2001**, *81*, 435–445.
- (40) (a) Lukat-Rodgers, G. S.; Rodgers, K. R. *Biochemistry* **1997**, *36*, 4178–4187. (b) Balland, V.; Bouzahir-Sima, L.; Kiger, L.; Marden, M. C.; Vos, M. H.; Liebl, U.; Mattioli, T. A. *J. Biol. Chem.* **2005**, *280*, 15279–15288.
- (41) Nagai, K.; Welborn, C.; Dolphin, D.; Kitagawa, T. *Biochemistry* **1980**, *19*, 4755–4761.
- (42) Ascenzi, P.; Brunori, M.; Coletta, M.; Desideri, A. *Biochem. J.* **1989**, *258*, 473–478.
- (43) Shiro, Y.; Iizuka, T.; Marubayachi, K.; Ogura, T.; Kitagawa, T.; Balasubramanian, S.; Boxer, S. G. *Biochemistry* **1994**, *33*, 14986–14992.
- (44) Jones, D. K.; Patel, N.; Raven, E. L. *Arch. Biochem. Biophys.* **2002**, *400*, 111–117.
- (45) Jeyarajah, S.; Proniewicz, L. M.; Bronder, H.; Kincaid, J. R. *J. Biol. Chem.* **1994**, *269*, 31047–31050.
- (46) Irwin, M. J.; Armstrong, R. S.; Wright, P. E. *FEBS Lett.* **1981**, *133*, 239–243.
- (47) Scott, E. E.; Gibson, Q. H.; Olson, J. S. *J. Biol. Chem.* **2001**, *276*, 5177–5188.
- (48) Chan, N. L.; Kavanaugh, J. S.; Rogers, P. H.; Arnone, A. *Biochemistry* **2004**, *43*, 118–132.

Table 2. Geometrical Parameters and Oxygen Affinities for the Staggered and Eclipsed Model Systems, with and without a H-Bond Acceptor. Distances in Angstroms, Angles in Degrees, Energies in kcal/mol

	Without H-Bond Acceptor		With H-bond Acceptor	
	eclipsed	staggered	eclipsed	staggered
$d_{\text{Fe-O}}$	1.774	1.777	1.777	1.846
$d_{\text{O-O}}$	1.288	1.288	1.290	1.293
$\angle\text{Fe-O-O}$	121.8	121.7	121.6	119.3
$d_{\text{Fe-N}\epsilon_{\text{Prox.His}}}$	2.139	2.119	2.133	2.122
ΔE_{O_2}	21.6	22.6	21.4	24.5

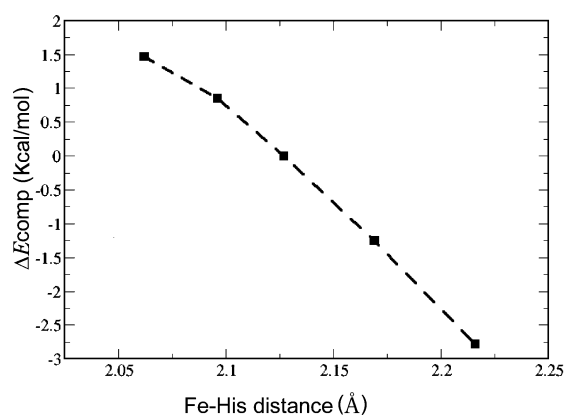
Fe–O bond. The balance of these opposing effects will determine the final Fe–O bond strength and the ΔE_{O_2} . From our results, it is evident that a carbonyl group as the proximal H-bond acceptor displays the optimal interaction that maximizes the benefits from both effects. It is interesting to note that proteins involved in oxygen transport (Mb, Hb, Lba, and several truncated hemoglobins) display carbonyl groups interacting with the proximal histidine. Last, as can be noted in Table 1, the use of the extended basis does not affect significantly the observed trends.

Contribution from the Proximal Histidine Conformation.

On the basis of the previous results that show the importance of H-bonding to the proximal histidine in determining O_2 affinity and in order to analyze the contribution of the His conformation, we calculated the oxygen affinity for two model systems (with and without a carbonyl H-bond to the $\text{N}\delta$) for the staggered and eclipsed conformations. The results are presented in Table 2. As we can see, there is a small difference (only +1 kcal/mol) between the staggered and the eclipsed configurations when the model system does not exhibit H-bond interactions. On the other hand, in the case in which a typical H-bond interaction is present, the difference favoring the staggered conformation is enhanced to 3 kcal/mol. This shows that proximal effects are not independent and that cooperative or synergistic effects can be expected.

Effect of the Fe–His Distance. To analyze the effect of the Fe–His distance on the oxygen affinity, we employed a model system consisting of a heme group with an imidazole ring coordinated by the $\text{N}\epsilon$ to the Fe. We then calculated the oxygen affinity as a function of the distance between the $\text{N}\epsilon$ of the proximal histidine and the porphyrin plane. A plot of the differences of the binding energy compared to the equilibrium distance value (ΔE_{comp}) against the Fe–His distance corresponding to each optimization is shown in Figure 4. The results show that the oxygen binding energy increases (up to 1.5 kcal/mol) when the His distance is constrained to smaller values than the optimal unconstrained value (2.12 Å), and that the binding energy decreases when the histidine is pulled away.

QM-MM Oxygen Affinity Calculation on Myoglobin and Leghemoglobin Wild-type and Mutants. The results presented in this work show that the three effects under study are operative in the modulation of oxygen affinity in heme proteins. The protein environment of the proximal histidine will determine the net effects, which may be decomposed in H-bond interactions to the proximal His, rotational position of proximal His, and Fe–His bond distance. As already mentioned in the Introduction, one paradigmatic case for proximal oxygen affinity regulation is Lba. Therefore, to further validate our conclusions in a more realistic system, we performed QM-MM calculations

**Figure 4.** Effect of the Fe–His distance on oxygen affinity.

on the relative oxygen binding energy of Lba and Mb. Relevant geometrical parameters for the QM-MM-optimized structures of the oxy proteins are shown in Table 3.

Visual inspection of the proximal environment shows that in Lba the $\text{N}\delta$ of the proximal histidine residue establishes a hydrogen bond with the carbonyl of LeuF4. In Mb, in addition to the CO-LeuF4, $\text{N}\delta$ also interacts with the OH of SerF7 (see Figure 5). The experimental values for the Fe–His stretching frequencies indicate an intermediate degree of charge relay from the histidine to the iron in both proteins. In Lba and Mb, the imidazole ring of the proximal histidine is attached to the protein by three sites: the covalent bond through histidine- $\text{C}\beta$, the H-bond interactions through its $\text{N}\delta$, and by coordination to the metal center. The relative position of these anchor points in the protein framework therefore determines the histidine rotational position and its distance to the porphyrin plane. The optimized structure reveals that in Lba the proximal histidine is in an optimal orientation for increasing O_2 affinity, which is evidenced by its relatively staggered rotational position and shorter Fe–His distance. On the other hand, in Mb, the histidine displays an eclipsed rotational position and a longer Fe–His distance. On the basis of the structural data, it is expected that in Lba the proximal effect has a notable positive influence on oxygen affinity, whereas an opposite effect is observed in Mb.

Distal cavities in Mb and Lba present important differences, too. Although in both cases there is a His residue (HisE7) close to the bound O_2 , it has been shown experimentally that mutation of HisE7xGly in Mb produces an important increase of the dissociation constant (~ 240 -fold), while in Lba, it remains almost invariant.¹⁶ This fact was proposed to be due to the presence of TyrB10 in Lba. The formation of a H-bond between the OH (TyrB10) and $\text{N}\delta$ of HisE7 leaves the His residue in a difficult position to stabilize the O_2 . Therefore, the distal His is only allowed to establish a weak H-bond with the O1 atom of the O_2 . This role of TyrB10 in sequestering the distal histidine has already been suggested based on experimental observations.¹⁶ On the other hand, in Mb, this position is occupied by a Leu residue (not shown in Figure 5) which is not able to produce this effect, so that HisE7 stabilizes the O_2 by a strong H-bond interaction with the O2 atom of the bound ligand.

To gain some insight into distal effects, we calculated the distal HisE7xGly mutants for Lba and Mb. The results confirm the fact that distal stabilization is more important in Mb⁴⁷ than in Lba.¹⁶ The decrease in the estimated oxygen binding energy barriers is about 7 and 3 kcal/mol for Mb and Lba, respectively.

Table 3. Geometrical Parameters, Charges Received by the O₂ (Δq_{O_2}) and Donated by the Proximal Imidazole (Δq_{Im}), and O₂ Relative Vertical Binding Energies ($\Delta(\Delta E_{O_2})$) for Wild-type and Mutants for the Oxy Complexes and of Wild-type and Mutants of Mb and Lba. Values in Parentheses Correspond to the RX Structure of Wild-type (wt) Mb.²² Distances in Angstroms, Angles in Degrees, Charges in e, Energies in kcal/mol.

	Myoglobin				Leghemoglobin			
	wt	HisE7xGly	HisF8xGly + Im.	double mutant	wt	HisE7xGly	HisF8xGly + Im.	double mutant
d_{Fe-O}	1.840 (1.935)	1.762	1.832	1.827	1.839	1.844	1.834	1.840
d_{O-O}	1.297 (1.223)	1.285	1.299	1.285	1.301	1.294	1.300	1.292
\angle_{Fe-O-O}	120.9 (118.2)	123.2	122.8	120.6	121.4	121.8	121.6	121.6
Δq_{O_2}	-0.214	-0.219	-0.286	-0.206	-0.302	-0.268	-0.302	-0.242
$d_{Fe-N\epsilon_{Prox.His}}$	2.183 (2.194)	2.178	2.098	2.094	2.041	2.047	2.038	2.066
dihedral _{Prox.His} ^a	78.4 (91.0)	76.6	56.4	65.3	60.1	58.9	72.6	79.4
Δq_{Im}	0.146	0.142	0.174	0.156	0.196	0.205	0.187	0.178
$\Delta(\Delta E_{O_2})^b$	0	-7.1	1.4	-4.7	0	-3.1	-1.6	-6.5
ν_{Fe-His}	221 ^c				223 ^d			
ν_{Fe-O_2}	570 ^e				576 ^f			

^a Dihedral_{Prox.His} refers to the angle between the plane of the proximal histidine imidazole and the line that goes through two opposite pyrrolic nitrogen atoms (N β and N δ) of the heme group. ^b Energy values with respect to the wild-type protein (kcal/mol). ^c From ref 43. ^d From ref 44. ^e From ref 45. ^f From ref 46.

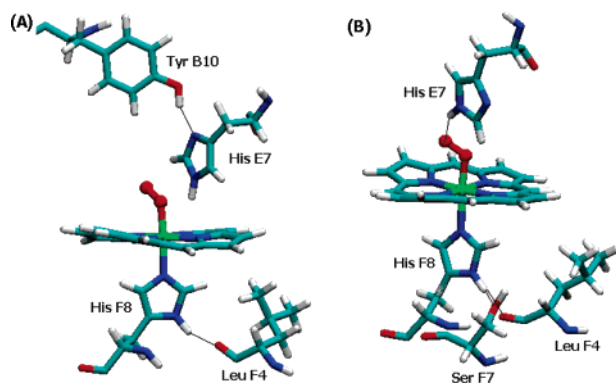


Figure 5. Active centers of leghemoglobin (A) and myoglobin (B).

Interestingly, in the HisE7xGly Mb mutant, the Fe–O distance is reduced to ~ 0.08 Å in HisE7xGly mutant compared to the wild-type protein, probably due to the loss of the strong H-bond interaction between O₂ and HisE7.

In order to quantify the proximal effects observed in Lba and Mb, we calculated the mutant protein HisF8xGly, in which we added an external imidazole coordinated to the Fe. This mutation has been obtained previously experimentally and led to a ~ 3 -fold increase in the k_{off} for Lba, while a ~ 3 -fold decrease was observed for Mb.¹⁷ The results presented in Table 3 show that indeed in Lba the mutation leads to a change in the dihedral angle so that now the histidine is closer to an eclipsed conformation. On the other hand, the Fe–His distance remains almost constant, while the hydrogen bond distance of the H δ –HisF8 with CO–LeuF4 reduces to about 0.1 Å. These results show that the imidazole of the proximal histidine is forced by the covalent attachment to the protein to be in a more favorable dihedral angle for oxygen binding, and when the covalent restraint is eliminated, the dihedral angle changes to a more eclipsed position, less favorable for O₂ binding but with a closer H-bond interaction. However, this covalent bond to the protein is not responsible for the very short Fe–His distance, as evidenced in the still very short Fe–His distance in the mutant protein. This last effect could be due to the strong proximal H-Bond with LeuF4 that fixes the His position very close to

the heme forcing the Fe–His distance to be about 0.08 Å shorter than that in the equilibrium distance for the isolated oxy complex. Summarizing the above, the proximal mutation leads to a rotation of the imidazole ring but does not affect the Fe–His distance. On the basis of the structural analysis, it is expected that the ΔE for oxygen release in HisF8xGly + imidazole (Lba) should be slightly lower than that for the wild-type protein. Consistently with this structural data and the experimental k_{off} values, a reduction of 1.6 kcal/mol in the oxygen binding energy was obtained for this mutant protein compared to that of the wild-type protein. In the case of Mb, as expected, the proximal mutation allows the proximal histidine to accommodate in a more favorable position for oxygen binding, which is observed in the reduction of Fe–His distance and in the rotational position of the proximal histidine, which becomes closer to the staggered conformation. As expected, the oxygen binding energy is now increased by 1.4 kcal/mol.

Finally, in order to check if the proximal effects are also operative in the absence of strong distal interactions, we calculated the double mutants HisE7xGly and His F8xGly + imidazole. In Mb, a low oxygen affinity is expected since distal stabilization is not present. However, due to the proximal mutation, the proximal histidine position is more favorable for oxygen binding, and the decrease in the O₂ binding energy is only 4.7 kcal/mol (compared to the 7.1 reduction in the distal mutant). In Lba, the opposite situation is obtained, and the binding energy is reduced by 6.5 kcal/mol (compared to the 3.1 reduction in the distal mutant). The structural trend in the imidazole rotational position and imidazole–iron distance is the same as that observed for the wild-type and HisF8 proximal mutant proteins discussed above.

Conclusions

Biological Implications. The Lba Case. Why is the O₂ affinity larger in Lba than in Mb, even when in Mb the distal stabilization is important and in Lba it is not? A possible answer to this question comes from an analysis of the relevant structural parameters for the QM-MM-optimized proteins. First, the Fe–His distance in Lba is small, almost 0.1 Å shorter than the

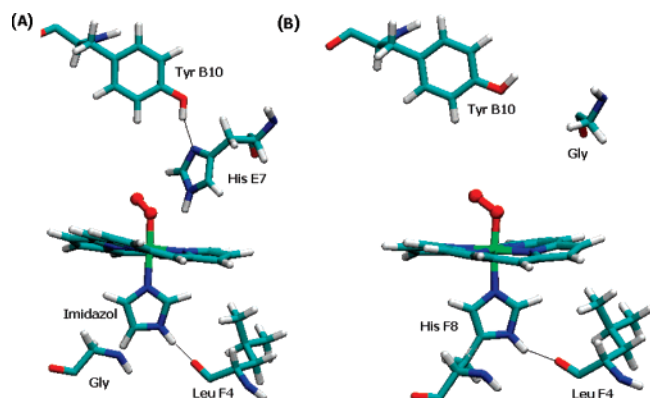


Figure 6. (A) Lba proximal mutant: HisF8xGly + imidazole. (B) Lba distal mutant: HisE7xGly.

equilibrium distance for the model system. This proves that in Lba the histidine residue is pulled up toward the heme group, reducing the Fe–His distance and enhancing the oxygen affinity. In Mb, on the contrary, the Fe–His distance is 0.06 Å longer than the isolated model equilibrium distance, and this probably means that the protein proximal environment in this case plays a completely opposite role than in Lba. Second, when comparing the dihedral angles in Mb and Lba, we observe that the histidine is close to the staggered conformation in Lba and to the eclipsed conformation in Mb, again pointing toward a proximal stabilization in Lba and destabilization in Mb. Last, since both proteins display similar H-bond interactions with the proximal histidine, no difference coming from charge relay effects is expected between them. However, as shown by our results, this effect enhances the contribution of the histidine rotational position to the O₂ binding.

Clearly, given that only a minor distal stabilization is present in Lba, the evolution selected a protein framework that positions the histidine close to the iron and in a staggered conformation, thereby increasing the oxygen affinity through proximal effects. On the other hand, in Mb, the opposite role of these effects seems to be the case.

Implications for Other Heme Proteins. Probably the most relevant case where proximal effects are also present is mammalian hemoglobin, where a drastic change in oxygen

affinity is observed due to a cooperative conformational change in the quaternary structure.⁹ Studies with hybrid non-iron-substituted hemoglobins revealed that the conformational change from the low affinity T-state to the high affinity R-state is accompanied by a reduction in the dissociation rate constant of about 50–100 fold for the α -subunits and about 20–60-fold for β -subunits.¹⁰ Whereas these differences have been attributed to changes in the distal pocket for the β -subunits, proximal effects are supposed to be responsible in the α -subunits.⁹ It is known that for the α -subunits in the T-state the proximal Fe–His bond is strained⁴⁸ (Fe–His bond distance of 2.6 Å)⁹ and relaxes when going to the R-state (Fe–His bond distance of 2.1 Å).⁹ Our results are able to explain the change in oxygen affinity in α -subunits of hemoglobin based on these observations. In the T-state, the hemoglobin pulls the proximal histidine away from the porphyrin, thereby decreasing oxygen affinity, and subsequently, the conformational change to the R-state frees the proximal histidine that becomes closer to the iron with the concomitant increase in O₂ affinity.

On model systems, our results show that proximal effects, which may be decomposed in charge relay, histidine conformation, and histidine–porphyrin distance effects are able to subtly modulate the oxygen binding energy and therefore the oxygen affinity. These effects are not independent and can work together or even compete. Regarding the proteins (Lba and Mb) and its mutants, our results are consistent with the experimental data on oxygen affinity. A detailed analysis of the proximal effects described herein is essential to understand the molecular basis of oxygen affinity in heme proteins since these effects could operate in a large variety of O₂ binding heme proteins.

Acknowledgment. This work was partially supported by the University of Buenos Aires, Agencia Nacional de Promoción Científica y Tecnológica (project PICT 06–08447), CONICET (PIP 02508), and Fundación Antorchas.

Supporting Information Available: Computational details of QM-MM calculations and optimized structures. This material is available free of charge via the Internet at <http://pubs.acs.org>.

JA0620033